Broadband Frequency Characterization of Optical Receivers Using Intensity Noise

Methods for enhancing the dynamic range of the intensity noise technique for high-frequency photoreceiver calibration are proposed and experimentally demonstrated. These methods combine recently developed EDFA* technology with spectral filtering techniques. The intensity noise calibration technique is portable, easy to use, and field deployable.

by Douglas M. Baney and Wayne V. Sorin

Optical technology will play an important role in building the coming information superhighway through its capacity to provide high information throughput and low-loss transmission simultaneously. Optical sources such as semiconductor lasers provide an optical carrier whose intensity is modulated with information to be sent over fiber-optic cable. For high-data-rate communications, lasers typically operate near the 1.55-μm or 1.3-μm low-loss wavelengths in optical fiber. Optical receivers convert the information modulated onto the optical carrier to baseband electrical signals. As demands are made for more information throughput, the bandwidths of optical receivers are increased commensurately.

Accurate characterization of the frequency response of an optical receiver is important to ensure that the receiver is compatible with the data transmission rate. Currently, a number of techniques exist to characterize the frequency response of optical receivers. One method is to compute the Fourier transform from the time-domain impulse response.[1] Frequency domain techniques, such as that used in the HP 8703 lightwave component analyzer, employ frequency-swept sinusoidal modulation of the optical intensity using a high-frequency $LiNbO_3$ modulator. This allows commercially available response measurements from 130 MHz to 20 GHz. The optical heterodyne technique using two Nd-YAG lasers has demonstrated capability from $\approx$10 MHz to 50 GHz at a wavelength of 1.32 μm.[1,2] These techniques all involve specific trade-offs among frequency coverage, experimental complexity, and sensitivity, and none are completely satisfactory. It is desirable to have the capability to measure the broadband frequency response with a simple rugged optical instrument.

The intensity noise technique offers the possibility of measuring frequency response characteristics of photoreceivers across the entire frequency span of modern electrical spectrum analyzers (for example, 9 kHz to 50 GHz for the HP 8565E). This intensity noise method was first demonstrated using a semiconductor optical amplifier as a source.[3] This technique is of particular interest because the noise exists at all frequencies simultaneously, permitting very rapid optical receiver characterization. Additionally, an unpolarized short-coherence-length optical source is used. This is advantageous

because it makes the measurements immune to polarization drifts and time-varying interference effects from multiple optical reflections, thereby allowing stable, repeatable measurements.

Intensity Noise Techniques

Intensity noise techniques take advantage of the beating between various optical spectral components of a broad-bandwidth spontaneous emission source. Any two spectral lines will beat, or mix, to create an intensity fluctuation with a frequency equal to the frequency difference between the two lines. This concept is illustrated in Fig. 1. Since the optical bandwidth of spontaneous emission sources can easily exceed thousands of gigahertz, the intensity beat noise will have a similar frequency content. The fluctuations in optical intensity are referred to as spontaneous-spontaneous, or sp-sp, beat noise.

There are many sources of broad-bandwidth spontaneous emission. Hot surfaces (such as tungsten light bulbs) can provide optical radiation ranging from the visible to the far infrared. Semiconductor sources such as edge emitting light-emitting diodes (EELEDs) provide increased power densities over a wavelength range of about 100 nm. Still higher power densities can be obtained from solid-state sources
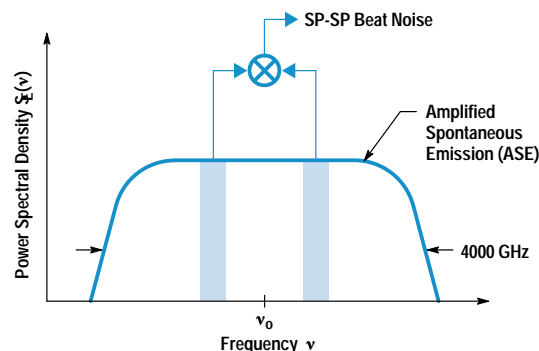
* Erbium-doped fiber amplifier.

Fig. 1. Spontaneous-spontaneous (sp-sp) beat noise arising from mixing of the various spectral components from a thermal-like optical noise source.
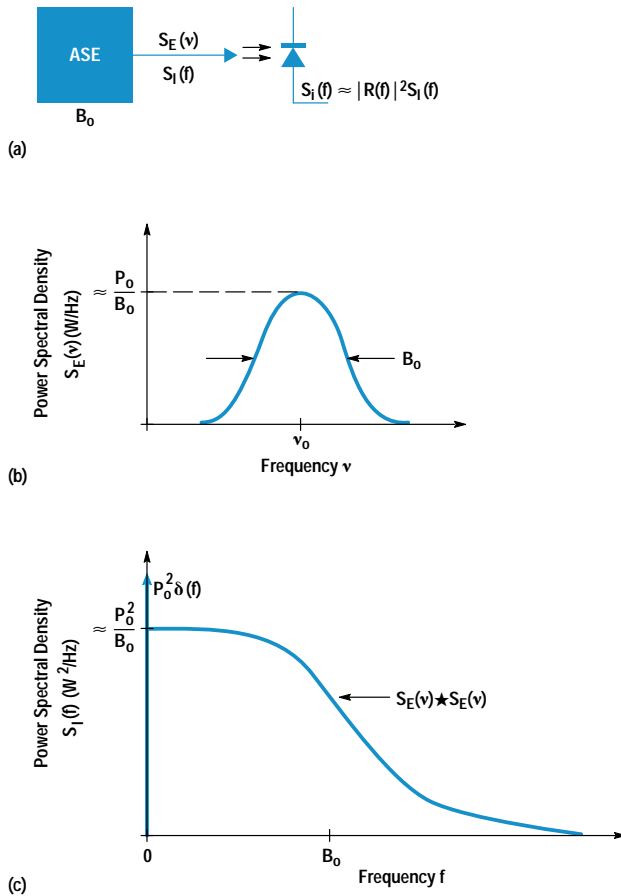
Fig. 2. (a) The intensity noise technique for optical receiver calibration. (b) The optical field spectrum as measured on an optical spectrum analyzer. (c) The optical intensity spectrum, which is proportional to the photocurrent spectrum, as measured on an electrical spectrum analyzer.

such as fiber-optic amplifiers (see page 9). The ability to couple these sources of broadband light efficiently into single-mode optical fiber is also important. Coupled power densities can range from about 500 pW/nm for a light bulb to greater than 1 mW/nm for amplified spontaneous emission (ASE) from a fiber-optic amplifier. The high power densities from fiber-optic amplifiers are particularly well-suited for intensity noise generation.

Bandpass-Filtered Intensity Noise Technique

Fig. 2 illustrates how the strength and line shape of the optical intensity beat noise are generated from a thermal-like source such as amplified spontaneous emission. Fig. 2a shows the optical power from an ASE source of spectral bandwidth B_O incident on the high-frequency optical receiver to be tested. The power spectral density of the optical field, $S_E(\nu)$, scaled so that its units are watts/Hz, is commonly used to characterize the output of optical sources. This quantity is typically measured using an optical spectrum analyzer. Fig. 2b shows a typical spectrum for $S_E(\nu)$ with full width at half maximum bandwidth B_O and center frequency ν_O. The average optical power P_O is found by integrating over the optical spectrum, that is,

$$P_O = \int_0^\infty S_E(\nu)d\nu,$$

which gives a peak value for the spectral density of approximately P_O/B_O. It should be noted that all power spectral densities discussed in this paper are single-sided, with energy only at positive frequencies.

Since photodiode current is proportional to optical intensity and not electric field, a more relevant quantity to consider is the power spectral density of the optical intensity, $S_I(f)$, which is scaled to have units of watts^2/Hz. This quantity is related to the optical field spectrum by the relatively simple expression:

$$S_I(f) = P_O^2\ \delta(f) + S_E(\nu) \star S_E(\nu), \tag{1}$$

where $\delta(f)$ represents a delta function and $\star$ denotes the single-sided autocorrelation (integrated over positive frequencies). This result assumes unpolarized ASE and single-sided power spectral densities. This expression is valid for optical radiation with thermal-like noise statistics, such as amplified spontaneous emission. The effects of shot noise are not included in equation 1 because it is easier to account for this noise after the optical intensity is converted to a photocurrent. The result of equation 1 is graphically illustrated in Fig. 2c. Intensity beat noise exists up to frequencies determined by the spectral width of the ASE source. These frequencies are typically on the order of thousands of gigahertz. The magnitude of the beat noise at low frequencies is approximately P_O^2/B_O, the exact value depending on the line shape of the electric field spectrum. More accurate values for typically encountered line shapes are given later.

The power spectral density of the detected photocurrent, $S_i(f)$, in units of amperes^2/Hz, equals that of the incoming intensity spectrum except for the filtering effects of the photodiode. If the frequency dependent responsivity (i.e., transfer function) for the photodiode is given by $R(f)$, which has units of amperes/watt, then the photocurrent spectrum can be expressed as:

$$S_i(f) \simeq |R(f)|^2 S_I(f) \tag{2}$$

The receiver thermal and shot noises are not included in equation 2. The value for these two noise sources will determine the SNR (signal-to-noise ratio) for the measurement technique. Assuming that the optical beat noise signal is larger than the shot or thermal noise, this expression can be used to determine the magnitude $|R(f)|$ of the frequency response of the photodiode. This measurement is performed by observing the photocurrent spectrum $S_i(f)$ with an electrical spectrum analyzer. If the spectral width of the ASE source, B_O, is much larger than the frequency response of the photodiode, then $S_I(f)$ can be assumed constant, and the responsivity squared $|R(f)|^2$ of the photodiode is displayed directly on the electrical spectrum analyzer.

One previous difficulty in the practical use of this detector calibration technique is the small value for the intensity beat noise provided by typical ASE sources. This has presented a problem for high-frequency calibration because the thermal noise level associated with wideband receivers is typically quite large. In this paper we show that by combining the recent development of erbium-doped fiber amplifiers with spectral filtering techniques, we can overcome the previous limitation of small signal strength.

To understand how to optimize the ASE for detector calibration, the concept of relative intensity noise or RIN, which has units of Hz^{-1}, will be introduced. This parameter can be thought of as the fractional intensity noise associated with an optical source. The definition for RIN in terms of the optical intensity spectrum is:

$$\text{RIN(f)} = S_I(f)/P_o^2. \qquad (3)$$

Thus RIN is the spectral density of the optical intensity at a given frequency divided by its integrated value at zero frequency. An equivalent definition equates RIN to the variance of the optical intensity $\langle \Delta I^2(f) \rangle$ in a one-hertz bandwidth divided by the average intensity squared. Since the optical bandwidth B_o is usually much larger than the electrical detection bandwidth, the RIN from an ASE source is usually considered to be constant, equal to its low-frequency value. From Fig. 2c, it can be seen that this value is approximately given by:

$$\text{RIN} \simeq 1/B_o. \qquad (4)$$

This result is valid for unpolarized light with thermal-like noise statistics. A more accurate value for equation 4 requires knowledge of the line shape of the ASE spectrum.

Normally, for a given source, one would increase the average optical power incident onto a photoreceiver to increase the photocurrent beat noise and hence the measurement sensitivity. With the development of EDFAs (erbium-doped fiber amplifiers), the average optical powers attainable will easily saturate high-frequency photoreceivers. This means increasing optical power is no longer an issue, and for a given optical receiver, a power just below its saturation level should be used for calibration purposes. Since incident optical power can now be considered a constant, depending on the detector saturation level, the concept of RIN becomes useful because increasing its value increases the SNR of the intensity noise technique. According to equation 4, this means that decreasing the spectral width B_o of the ASE source will improve the SNR for detector calibration. The only limitation is that eventually there will be a roll-off in the high-frequency content of the beat noise.

Effects of Line Shape and Bandwidth

As the optical bandwidth is reduced, the maximum frequency separation of beating components also decreases. In Fig. 3, the RIN is shown as a function of frequency for four
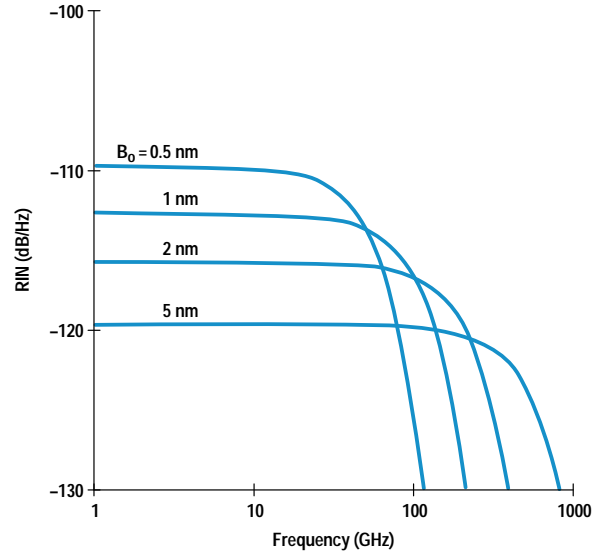

Fig. 3. Relative intensity noise (RIN) for a Gaussian-shaped optical field power spectrum centered at 1.55 μm.

different optical bandwidths. The plotted curves correspond to the case of an unpolarized ASE source with a Gaussian optical spectral shape. The highest RIN is achieved at the lowest frequencies with the narrowest optical bandwidth. At frequencies comparable to the optical spectral bandwidth, roll-off in the RIN becomes apparent. The RIN for the 5-nm spectral width is relatively constant to several hundred gigahertz. Expressions for RIN as a function of frequency are shown in Table I for the case of Lorentzian, Gaussian, and rectangular optical field spectrums. The Lorentzian shape corresponds closely to the spectrum of commonly used Fabry-Perot optical filters. The Gaussian spectrum is sometimes used to describe the spectra of EELEDs or lasers operating below threshold. The rectangle function approximates some interference filters, grating-based monochromators, and chirped fiber gratings. The normalized (to unity) optical field spectrum is also included in Table I for reference. The line width B_o in each case is the FWHM (full width at half maximum) of the optical field spectrum.

Comparing the low-frequency RIN values for each of the different spectral shapes, the rectangle spectrum delivers the most RIN ($1/B_o$), followed by the Gaussian ($0.66/B_o$),

Table I
Relationship between Unpolarized Optical Field Spectrum and RIN

Optical Field Spectrum Shape	Normalized $S_E(\nu)$	RIN(f) (f > 0)
Rectangle*	$\prod\left(\dfrac{\nu - \nu_o}{B_o}\right)$	$\dfrac{1}{B_o}\bigwedge\left(\dfrac{f}{B_o}\right)$
Gaussian	$\exp\left\{-(4\ln 2)\left(\dfrac{\nu - \nu_o}{B_o}\right)^2\right\}$	$\dfrac{1}{B_o}\dfrac{\sqrt{2\ln 2}}{\sqrt{\pi}}\exp\left\{-(2\ln 2)\left(\dfrac{f}{B_o}\right)^2\right\}$
Lorentzian	$\dfrac{1}{1 + 4\left(\dfrac{\nu - \nu_o}{B_o}\right)^2}$	$\dfrac{1}{B_o}\dfrac{1}{\pi}\dfrac{1}{1 + (f/B_o)^2}$

* $\prod$ = rectangle function. $\bigwedge$ = triangle function.

1.55-μm Fiber-Optic Amplifier

The fiber-optic amplifier is a key element in modern high-data-rate communications. Its large optical bandwidth, ≈ 4000 gigahertz, makes it effectively transparent to data rate and format changes, allowing system upgrades without modifications to the amplifier itself. The most prevalent fiber-optic amplifier is called the erbium-doped fiber amplifier (EDFA). It provides amplification in the third telecommunications window centered at a wavelength of 1.55 μm. The EDFA has four essential components, as shown in Fig. 1. These are the laser diode pump, the wavelength division multiplexer (WDM), the erbium-doped optical fiber, and the optical isolators. To achieve optical amplification, it is necessary to excite the erbium ions situated in the fiber core from their ground state to a higher-energy metastable state. A diagram of the relevant erbium ion energy states is shown in Fig. 2. The erbium ions are excited by coupling pump light (≈ 20 mW or greater) through the WDM into the erbium-doped fiber. Commonly used pump wavelengths are 980 nm and 1480 nm. The ions absorb the pump light and are excited to their metastable state. Once the ions are in this state, they return to the ground state either by stimulated emission or, after about 10 ms, through spontaneous emission. Light to be amplified passes through the input isolator and WDM and arrives at the excited erbium ions distributed along the optical fiber core. Stimulated emission occurs, resulting in additional photons that are indistinguishable from the input photons. Thus, amplification is achieved. Optical isolators shield the amplifier from reflections that may cause lasing or the generation of excess amplified spontaneous emissions (ASE).

Good EDFA design typically requires reduction of optical losses at the amplifier input and minimizing optical reflections within the amplifier. EDFAs with greater than 30-dB optical gain, more than 10-mW output power, and less than 5-dB noise figure are readily achieved in practice.
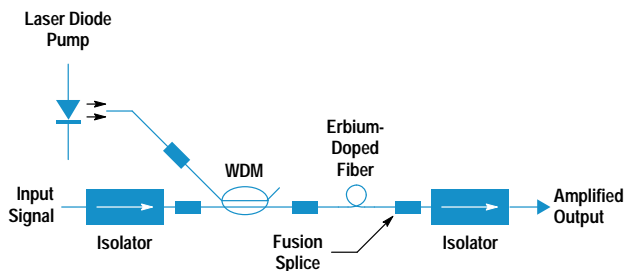

Fig. 1. Schematic of an erbium-doped fiber amplifier showing essential optical components. The WDM is a wavelength division multiplexer.

Fig. 2. Relevant erbium ion energy levels.

ASE is generated in optical amplifiers when excited ions spontaneously decay to the ground state. The spontaneously emitted photons, if guided by the optical fiber, will subsequently be amplified (by the excited ions) as they propagate along the fiber. This can result in substantial ASE powers (>10 mW) at the amplifier output. A typical spectrum of signal and ASE at the amplifier output is shown in Fig. 3. The ASE can extend over a broad spectral range, in this case in excess of 40 nm.

Fig. 3. Spectrum of amplified spontaneous emissions (ASE) and amplified signal at the amplifier output.

and next by the Lorentzian ($0.32/B_O$). If the ASE source is polarized, the RIN will be twice as large for all three cases.

If the optical receiver response measurements are performed in the flat RIN regime (see Fig. 3), no specific knowledge of the source line shape is required. However, if the spectral line shape for the ASE source is accurately characterized, additional measurement sensitivity can be obtained by using narrower optical filters and correcting for the roll-off in the response data.

Experiment: Intensity Noise Technique Using Optical Bandwidth Reduction

To demonstrate the filtered intensity noise technique, measurements were performed at a wavelength of 1.55 μm on a SONET receiver with 1-GHz electrical bandwidth. The measurement setup is shown in Fig. 4. The mirror at the end of the EDFA results in two-pass ASE generation. This doubly amplified ASE is then filtered by an optical bandpass filter with a 1-nm spectral width. All optical connections were fusion-spliced to eliminate optical reflections. The presence
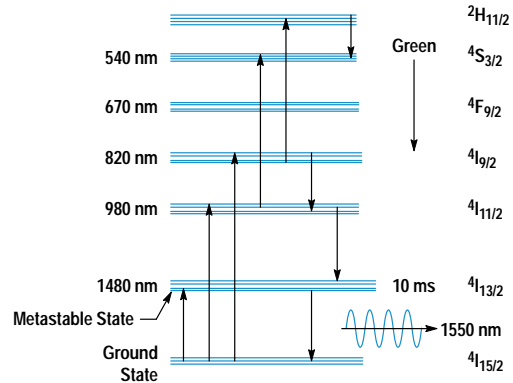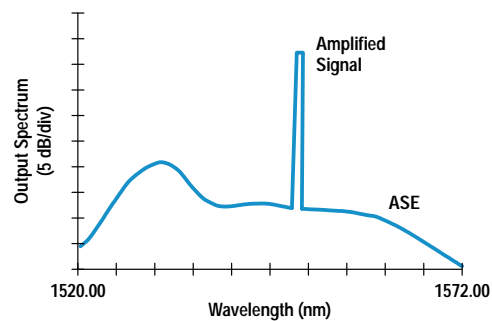
of multiple optical reflections could impart undesirable intensity ripple onto an otherwise constant RIN spectrum, which would be difficult to separate from the receiver frequency response. The bandpass filtering resulted in approximately a 15-dB improvement in SNR. An average optical power of 200 μW was incident onto the receiver; this was below its saturation level of 320 μW. Using a more complicated dual Nd-YAG optical heterodyne system, measurements at a wavelength of 1.32 μm were performed for comparison with the intensity noise technique. The intensity noise technique shows excellent agreement when compared with the standard heterodyne method as indicated in Fig. 5.

Periodically Filtered Intensity Noise Technique

As discussed earlier, for a fixed average optical power, the spontaneous-spontaneous beat noise in the photocurrent spectrum increases as the optical bandwidth B_O is reduced. This increase in signal strength is desirable, but if the optical bandwidth is reduced too much, the high-frequency content of the beat noise will start to roll off, making it unsuitable
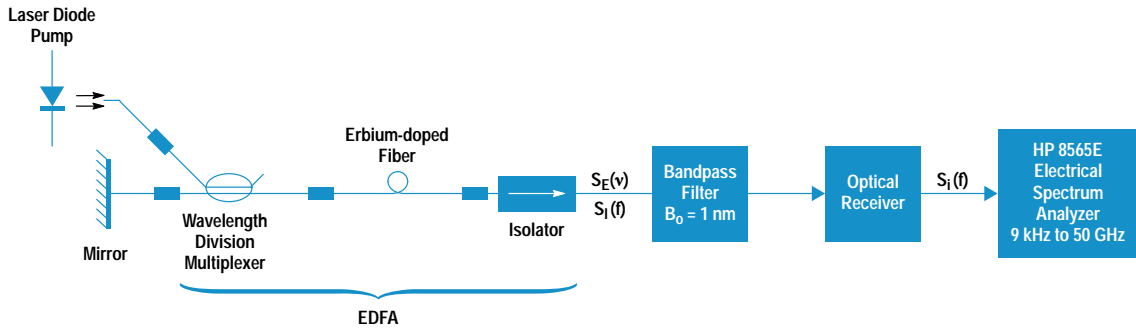
Fig. 4. Experimental arrangement for frequency response measurement of a SONET photoreceiver using the bandpass-filtered intensity noise technique.

for high-frequency detector calibration. In practice, this trade-off between signal strength and frequency content becomes a problem when trying to characterize high-frequency, low-gain optical receivers. Because of the large input noise figures (typically 30 dB) associated with high-frequency electrical spectrum analyzers, large values of photocurrent beat noise are required.

The periodically filtered intensity noise technique solves this trade-off problem by allowing the magnitude of the beat

Fig. 5. Measurement of a SONET receiver frequency response using (a) a 1.32-μm Nd-YAG optical heterodyne system and (b) the 1.55-μm filtered intensity noise technique.

noise to be increased without loss of its high-frequency content.[4] This is accomplished by passing the amplified spontaneous emission through a Fabry-Perot filter and then on to the high-frequency optical receiver. This reduces the average optical power while maintaining the magnitude of the spontaneous-spontaneous beat noise at periodic frequencies spaced at intervals equal to the free spectral range of the filter. The result is an increase in RIN at periodically spaced beat frequencies. If needed, optical amplification can then be used to boost the average optical power to a value just under the saturation level for the receiver.

Details of the periodically filtered technique are shown in Fig. 6. Fig. 6a shows the ASE from a source such as an erbium-doped fiber amplifier passing through a Fabry-Perot filter and on to the test optical receiver. The transmission characteristics of the Fabry-Perot filter are determined by its free spectral range, FSR, and its finesse, F. FSR is the frequency separation of the transmission maxima and F is the ratio of the FSR to the width of the transmission maxima. From a signal processing point of view, the Fabry-Perot filter has a frequency-domain transfer function for the optical field given by $H(\nu)$. The squared magnitude of this transfer function is illustrated in Fig. 6b. For the ideal case, the transmission through the filter would be unity at frequencies separated by the FSR. After passing through the filter, the power spectral density of the input optical field $S_E(\nu)$ will be transformed to $|H(\nu)|^2 S_E(\nu)$. Fig. 6c shows the filtered spectrum, which is incident on the optical receiver. Strong beat signals occur in the intensity separated by frequency intervals equal to the FSR of the Fabry-Perot filter. As described earlier in equation 1, the power spectral density for the optical intensity $S_I(f)$ can be obtained from an autocorrelation of the input electric field spectrum:

$$S_I(f) \simeq P_O^2 \delta(f) + |H(\nu)|^2 S_E(\nu) \star |H(\nu)|^2 S_E(\nu). \quad (5)$$

This expression is valid for unpolarized amplified spontaneous emission (see equation 1). The result of equation 5 is illustrated in Fig. 6d. Intensity noise peaks are evident at frequency locations separated by the FSR of the Fabry-Perot filter. Relative to the dc signal, these peaks are a factor of F/π larger than the unfiltered case shown in Fig. 2c. For a typical finesse of F = 100, this corresponds to an increase in signal-to-noise ratio of about 15 dB for photodiode characterization. The penalty for the increased SNR is that beat signals only occur at specific frequencies. This constraint is not very severe because this frequency spacing can be set to any
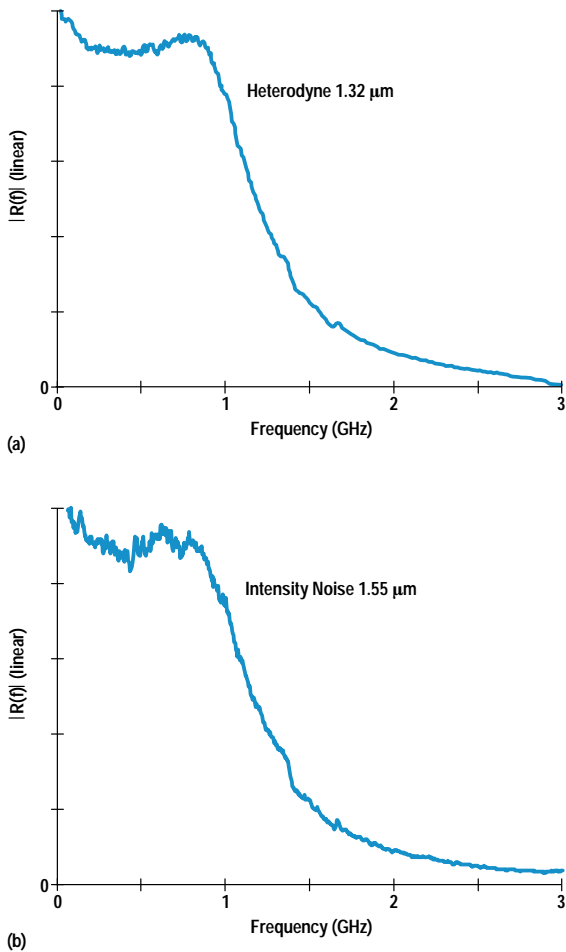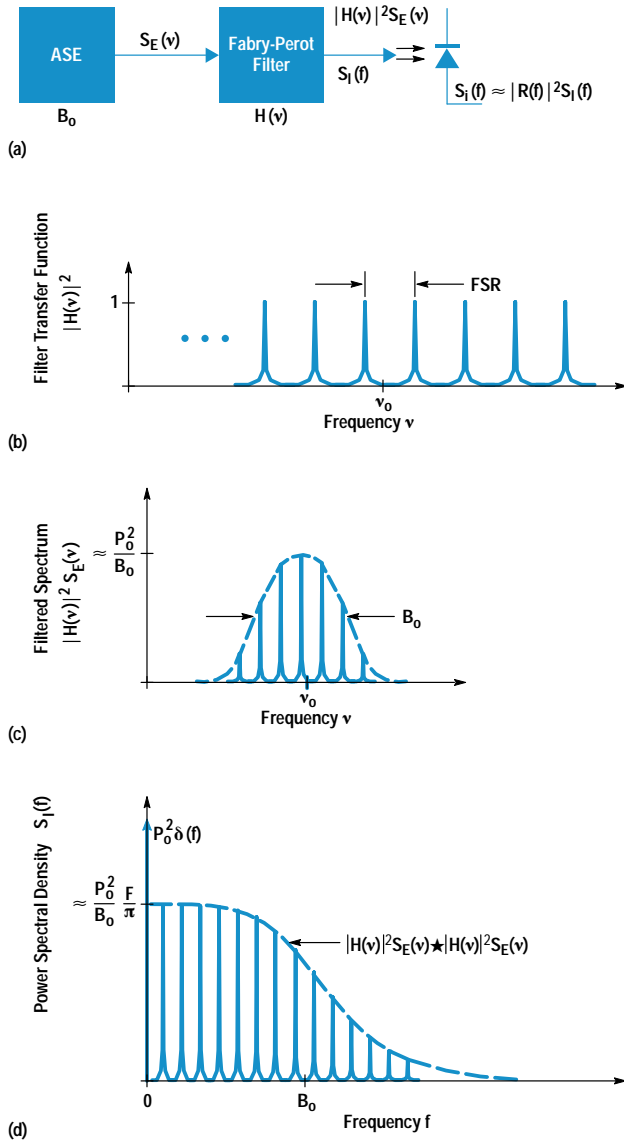
Fig. 6. (a) Block diagram illustrating the periodically filtered intensity noise calibration technique. (b) Transfer function of the Fabry-Perot filter. (c) Optical field spectrum incident at the photoreceiver. (d) Photocurrent spectrum as measured on an electrical spectrum analyzer.

desired value by proper choice of the filter FSR. As described earlier, the optical receiver frequency response can be obtained using equation 2, which relates the optical intensity spectrum to the photocurrent spectrum measured using an electrical spectrum analyzer. Assuming an optical bandwidth B_O much larger than the frequency response of the optical receiver, the photocurrent power spectrum is given by:

$$S_i(f) \simeq |R(f)|^2 S_I(f) = |R(f)|^2 \frac{P_O^2}{B_O} \cdot \frac{F}{\pi} \sum_k \frac{1}{1 + \left(\frac{f - kFSR}{\Delta\nu}\right)^2}$$

where $\Delta\nu$ is the spectral width of the Fabry-Perot filter and is given by $\Delta\nu = FSR/F$. This result illustrates that the magnitude of the photocurrent beat signal can be increased relative to a fixed average current without sacrificing its high-frequency content.

Experiment: Intensity Noise Technique Using Periodic Bandwidth Reduction

To demonstrate the above result, the arrangement illustrated in Fig. 7 was used. The ASE obtained from the two-pass EDFA superfluorescent source generated an optical signal with a spectral width of about 40 nm centered at 1.55 μm. This ASE then passed through an optical isolator, which prevented the two-pass superfluorescent source from becoming a laser. The output of the isolator was then sent through a single-mode fiber Fabry-Perot filter with finesse F = 80 and free spectral range FSR = 680 MHz. To boost the average power, the filter output was optically amplified by a final EDFA postamplifier. Average output powers of several milliwatts can be obtained using this arrangement. Fusion splices between the superfluorescent source, the filter and the postamplifier were used to minimize reflections. This is important because multiple reflections will add amplitude ripple to the intensity power spectrum. The photoreceiver consisted of a high-speed 14-μm-diameter, InGaAs p-i-n photodiode followed by a traveling wave GaAs microwave amplifier. A 50-GHz electrical spectrum analyzer (HP 8565E) displayed the photocurrent power spectrum.

For comparison purposes, three different techniques were used to measure the frequency response of the photoreceiver. The results of these three measurements are shown in Fig. 8. The curve labeled A was obtained using unfiltered ASE. For
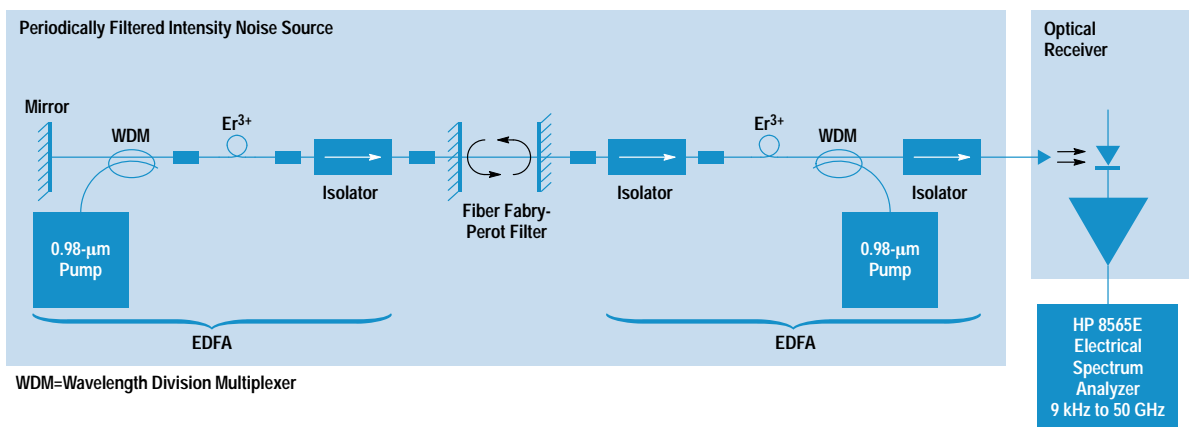

Fig. 7. Experimental setup used to demonstrate the periodically filtered intensity noise technique.
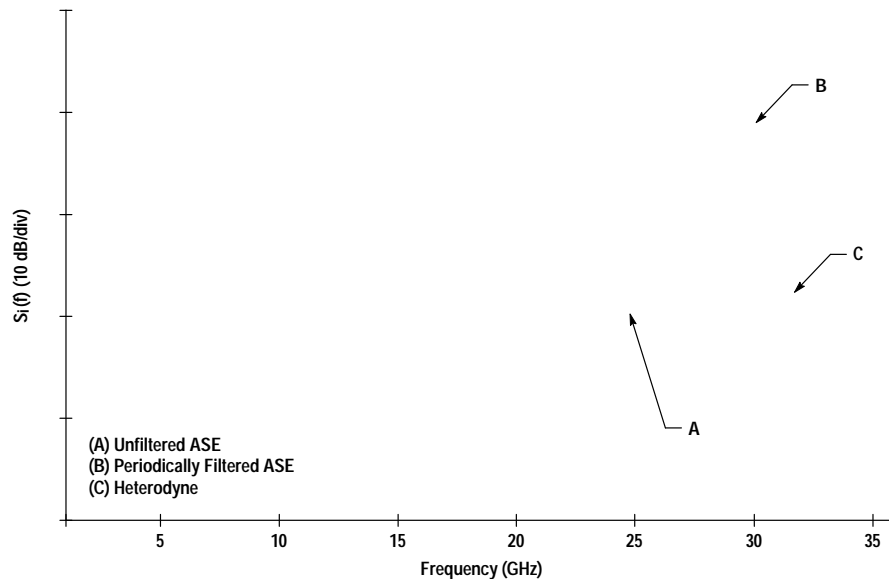
Fig. 8. Frequency response measurements of a high-frequency optical receiver using three techniques. The intensity noise curves were measured at 1.55 μm and the heterodyne measurement was made at 1.32 μm.

curve B, the periodically filtered ASE output was used. The average optical powers were held constant and equal for curves A and B. Curve C was generated using an optical heterodyne technique. Curves A and B experimentally demonstrate an SNR enhancement of approximately 17 dB between the filtered and unfiltered intensity noise techniques. Comparison between the heterodyne technique and the two intensity noise techniques shows very good agreement, illustrating the flat intensity noise spectrum obtained from the EDFA noise source.

Discussion

The use of a broadband intensity noise source for high-frequency detector calibration has several advantages over other frequency-domain techniques. One important advantage is that calibration of the frequency response of the optical source is not necessary since it can be made flat by choosing the ASE spectral width to be much larger than the frequency response of the photodetector. This is not the case for other frequency-domain techniques. For example, sinusoidal intensity modulation of an optical source using a $LiNbO_3$ modulator requires careful calibration of the frequency response of the modulator, which becomes increasingly difficult at high frequencies. Any errors in this calibration are passed on to the detector's frequency response.

Compared with heterodyne techniques, the intensity technique is rugged and field deployable and does not require stable polarization alignment. Since the intensity noise is present at all frequencies, it allows rapid measurements. Additionally, the long coherence length of laser sources in the presence of optical reflections makes the heterodyne measurement more susceptible to environmental effects.

The intensity noise method also has advantages compared to time-domain impulse measurement methods. For high-frequency measurements, the effects of the oscilloscope must be deconvolved from the measurement before an accurate calibration can be obtained. This can often be arduous since accurate impulse responses for high-frequency oscilloscopes are difficult to obtain. The advantage of not requiring careful

source calibration for the intensity noise technique is an important consideration in developing a portable, low-cost, user-friendly calibration technique.

Summary

In this paper we have proposed and experimentally demonstrated methods for enhancing the dynamic range of the intensity noise technique for high-frequency photoreceiver calibration. By combining recently developed EDFA technology with spectral filtering techniques, we have shown that the magnitude of intensity beat noise can be increased to values practical for unamplified photodiode calibration. Using the periodically filtered technique, RIN values larger than −100 dB/Hz can be achieved over a frequency range in excess of 100 GHz. The intensity noise calibration technique has the potential for becoming a portable, easy to use, field deployable calibration method.

Acknowledgments

References

1. D.J. McQuate, K.W. Chang, and C.J. Madden, "Calibration of Lightwave Detectors to 50 GHz," *Hewlett-Packard Journal,* Vol. 44, no. 1, February 1993, pp. 87-91.

2. S. Kawanishi, A. Takada, and M. Saruwatari, "Wideband Frequency-Response Measurement of Optical Receivers Using Optical Heterodyne Detection," *Journal of Lightwave Technology,* Vol. 7, no. 1, 1989, pp. 92-98.

3. E. Eichen, J. Schlafer, W. Rideout, and J. McCabe, "Wide-Bandwidth Receiver/Photodetector Frequency Response Measurements Using Amplified Spontaneous Emission from a Semiconductor Optical Amplifier," *Journal of Lightwave Technology,* Vol. 8, no. 6, 1990, pp. 912-916.

4. D.M. Baney, W.V. Sorin, and S.A. Newton, "High-Frequency Photodiode Characterization Using a Filtered Intensity Noise Technique," *IEEE Photonics Technology Letters,* Vol. 6, no. 10, October 1994, pp. 1258-1260.